TEMPERATURE-DEPENDENT MECHANICAL RESPONSE OF CARBON NANOTUBE REINFORCED EPOXY NANOCOMPOSITES: AN ATOMISTIC SIMULATION STUDY

Jacob Schichtel, Bonsung Koo, Aditi Chattopadhyay

Arizona State University
Tempe, Arizona

ABSTRACT

A preliminary analysis of the temperature-dependent elastic and plastic response of carbon nanotube (CNT) reinforced nanocomposites using an atomistically informed approach is presented. By utilizing molecular dynamics (MD) simulations, the effects of temperature on mechanical properties have been investigated for epoxy-based polymer composites reinforced by randomly dispersed CNTs. A molecular model has been developed for the bulk matrix of the randomly dispersed CNT architecture, and virtual deformation tests have been performed to estimate mechanical properties under a wide range of temperatures. The results indicate that the strength and stiffness of these nanocomposites degrade as the temperature increases and the increase in temperature is linked to an increase in the Poisson's ratio. This physics-based understanding of the effects of temperature and nanoconfiguration on critical mechanical properties will be valuable for the design optimization of nanocomposites.

1. INTRODUCTION

Carbon nanotube (CNT) reinforced epoxy-based nanocomposites are widely known to have exceptional material properties at standard temperatures. On its own, cured epoxy resins have remarkable adhesive strength, high heat and chemical resistance, versatile manufacturability and relatively low cost. Properties can be tailored depending on the specific chemical structure, curing agents used, and curing conditions. However highly crosslinked epoxies are limited in their use for structural applications by their inherent brittleness [1],[2]. CNTs have sparked great research interest due to their unprecedented theoretical mechanical, thermal, and electronic properties. Their aspect ratio is unparalleled with single walled CNTs having diameters from less than 1 nm to over 100 nm and lengths on the order of μm to mm. The strength and stiffness of individual CNTs surpass that of carbon fibers, exhibiting a Young's modulus over 1000 GPa and tensile strength up to 63 GPa [3]. These impressive properties make them a promising reinforcing material for epoxy-based composites. Though their tendency to agglomerate can diminish their advantages, with a critical weight percentage and uniform dispersion of CNTs in an epoxy matrix, these nanocomposites can demonstrate improved strength and stiffness over neat matrix, as well as significantly improved toughness. The CNT interfacial crack propagation mechanisms help to offset the brittleness of neat epoxy [4],[5],[3],[1]. Thus, these advanced nanocomposites are attractive materials for engineering applications such as adhesives and aerospace components [1],[6]. In order to expand their use beyond room temperature applications, is important to understand the effects of temperature on the mechanical properties of nanocomposites.

SAMPE Conference Proceedings. Charlotte, NC, May 20-23, 2019. Society for the Advancement of Material and Process Engineering – North America.

Thermoset polymers such as epoxy generally have better performance at relatively high temperatures than thermoplastics because of their crosslinks; however, they are still limited as their mechanical properties degrade near their glass transition temperature (Tg). Allaoui et al. studied the effect of CNTs on the Tg but were unable to find a lucid connection [7]. Studies on the temperature-dependent properties of epoxy polymers with nanoreinforcements are limited. Foreman et al. showed good prediction of thermomechanical properties for neat epoxy using Group Interaction Modelling [8], but these models do not incorporate the effects of nanofiller reinforcements. For nanoclay reinforced polymeric nanocomposites, Bayar et al. studied the effects of temperature and reinforcement percentages on the Young's modulus and the Poisson's ratio [9], but more work needs to be done to expand these results to a wider set constituents and understand the underlying mechanisms.

Due to the architecture of CNT reinforced nanocomposites, the fundamental mechanisms must be captured on the nanoscale. Previous work performed by Koo et al. has estimated the Tg point of neat epoxy and smart polymer systems with high accuracy using atomistic simulations [10], but this work has not yet incorporated the effects of nano-inclusions or the estimation of mechanical properties at temperatures approaching the Tg. Molecular simulations of the mechanical properties of a polyimide composite with carbon nanotubes have been performed showing favorable changes in strength and stiffness at two separate temperatures compared to neat polyimide. However, the results of this study are likely skewed by the unrealistically high weight percentages of CNT indicated by CNT counts and system size (though unspecified) [11]. In fact, due to computational limitations many MD simulations involving CNT reinforced composites utilize unrealistically high CNT weight percentages, which inevitably induces inflated results [12]. Therefore, there is a need to study the effects of CNTs and temperature on the mechanical properties of nanocomposites at the fundamental length scale using more reasonable molecular systems. In this study we have modeled the crosslinked bulk epoxy matrix imbedded with randomly dispersed CNTs and captured its thermal degradation. MD deformation tests have been performed to estimate mechanical properties under an extensive range of temperatures.

2. MODEL DEVELOPMENT

2.1 Representative unit cell for randomly dispersed CNT nanocomposite

In this study, diglycidyl ether of bisphenol-F (DGEBF) also known as EPON 862, one of the most common epoxy resins [13], was used for the matrix with the curing agent, diethylenetriamine (DETA). Our representative unit cells (RUCs) comprised 1,069 DGEBF molecules, 874 DETA molecules, and two single-walled chiral (10, 5), 3.8 nm long CNTs with hydrogenated ends for a total of 64,407 atoms using the Packmol initial configuration software [14], thus maintaining the experimental weight ratio of 100:27 for DGEBF to DETA [15] and a CNT weight percentage of 2.5 %. The geometric coordinate files for the resin and hardener were produced using Open Babel [16], and five distinct RUCs were randomly generated with unique seed numbers, so that average values across the systems could be used to improve the accuracy of calculations. One of these systems is shown in figure 1 in its post-crosslinking state. As is standard in MD simulations for mechanical properties, periodic boundary conditions were utilized to mitigate edge artifacts and allow bonds to form across the boundaries, thus forming a better representation of the bulk material.

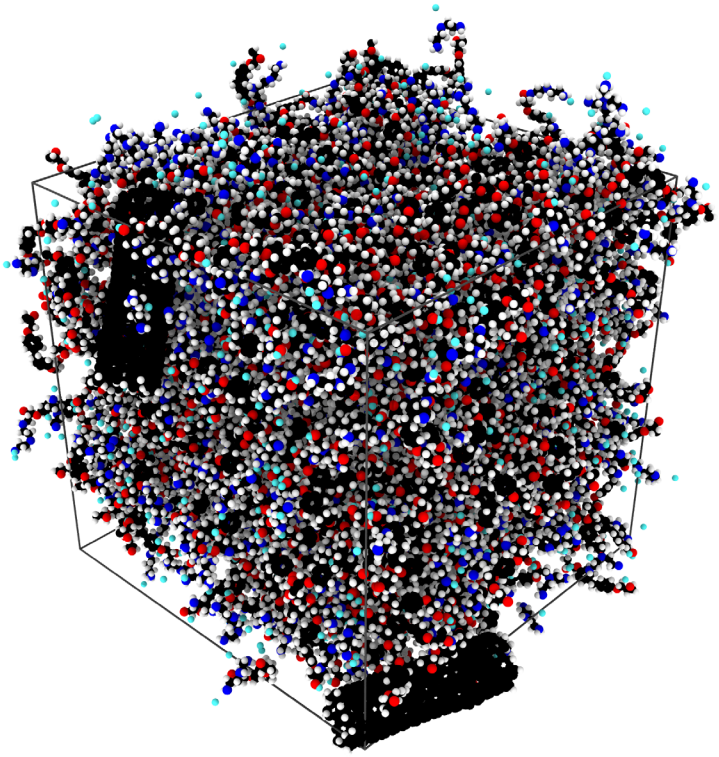

Figure 1. Example RUC showing two CNTs randomly dispersed in a highly crosslinked epoxy matrix. Note that by the nature of the periodic boundaries, bonds are formed across the RUC and around the CNTs.

In practice, CNT weight fraction is generally not greater than 1% due to CNT agglomeration; however, in this study a CNT weight percentage of 2.5% was used to dramatically reduce the required system size while still maintaining a reasonable CNT weight percentage with more than a single CNT. Moreover, since CNTs essentially reside in both the nanoscale and the microscale, the aspect ratio of the CNTs in our RUC is considerably smaller than that of full length CNTs. However, the four alternative solutions introduce larger issues. Creating a theoretically infinitely long CNT that bonds across the periodic boundary does not allow any CNT bending or reorientation, and heavily biases the mechanical properties in a particular direction. Inserting CNTs with unrealistically small diameters alters the CNT/matrix interactions while still not achieving characteristic aspect ratios. Reducing the number of CNTs to one and trying to justify random dispersion by averaging over a series of RUCs with a single randomly placed CNT completely disregards any interactions between individual CNTs. Finally, simply increasing CNT lengths without regard for MD limitations either imposes immoderate CNT weight percentages or necessitates an unreasonably large system size, inducing insurmountable computational costs. Therefore, the RUC developed prudently balances the many variables and constraints for a reasonable molecular model of epoxy imbedded with randomly dispersed CNTs; however, it should be noted that the limited aspect ratio of these CNTs may underestimate the mechanical property improvements caused by the introduction of CNTs into the composite.

2.2 Development of highly crosslinked epoxy polymer

The Large-scale Atomic/Molecular Massively Parallel Simulator (LAMMPS) was used for all molecular dynamics simulations [17]. A classical force field, the Merck Molecular Force Field (MMFF) was used for the resin and hardener molecules; the parameters were generated from SwissParam [18] and reformatted for use in LAMMPS. Parameters from the OPLS force field were used for the CNTs [19]. CNT connectivity was established using VMD TopoTools [20], and periodic boundary conditions were applied in all directions.

A stochastic proximity-based crosslinking method was utilized to create a complex 3D polymer network using the novel bond/react algorithm developed by Gissinger et al. [21]. Energy minimization was initially conducted using the conjugate gradient method. Subsequently, network creation was performed over 100,000 femtosecond timesteps in an NPT ensemble enforced by the Nose/Hoover thermostat and barostat. The pressure was set to 1 atm and 400K to emulate basic curing conditions. The properties of a cured epoxy have been shown to be dependent on the curing temperature [22], so the crosslinking was simulated at 400K to match the elevated curing temperatures [1], [23], [24]. As a result of the instantaneous increases in potential energy resulting from sudden topology changes, the temperature increased to 450K when the rate of crosslinking was the highest. This parallels the increase of temperature that naturally occurs during actual crosslinking due to the exothermic reactions, though the actual mechanisms for the increase in kinetic energy differ. The bond formation was set to occur when the distance between eligible bonding atoms falls below 3.25 Å, which is the addition of the carbon and nitrogen Van der Waals radii. Bond, angle, dihedral, and improper bonding information and the partial charges were appropriately updated for each crosslink formed, followed by a period of 100 timesteps of energy minimization to relax high energy configurations. The choice of 100 timesteps was selected after running several test simulations to limit the minimization period while eliminating instabilities.

This crosslinking method provides several advantages over typical MD crosslinking techniques including allowing the continuous formation of bonds in an NPT ensemble and preserving the true topology of unreacted portions of molecules. In addition, it can expediate the density equilibration process thereby decreasing computational costs. Nevertheless, it is important to mention that while this method efficiently produces a crosslinked system using an intuitive procedure, it is not meant to mimic the distinct reaction physics and diffusion of macroscale curing. Crosslinking speed is typically limited by diffusion [25], causing cure times to be on the order of minutes to days. Because of our system's scale and the fact that is initiated in a randomly dispersed state, the curing process is comparatively instantaneous. For our purposes these details are not necessary, since for our study we are interested in the end result: a stochastically crosslinked stable 3D network.

The density of the systems increased to an average of 0.985 g/cm^3 (at 400K), and an average crosslinking degree of 97.1 %. This degree of curing is higher than often desired for engineering applications, but it is not unreasonable. Sinclair achieved curing degrees approaching 1 at elevated temperatures near 400K. Yang et al. measured the degree of curing for a bisphenol-A epoxy to be 97.89 % [26] and Carrasco et al. managed to measure epoxide conversion rates of up to 98.7 % for a trifunctional epoxy resin [27]. Visco et al. also observed high resin conversion of up to 96 % with 1.5 weight percent CNT [28]. All achieved asymptotically plateauing degrees of curing similar to that of our MD simulations as shown in Figure 2, despite the timescale difference. Furthermore, crosslinking density is not homogenous throughout the epoxy, so even in epoxies

with lower degrees of curing, local regions of higher crosslinking density must exist and are likely important for load bearing. Future work may be performed at varying crosslinking degrees by stopping the crosslinking at a certain threshold or crosslinking at lower temperatures, but for this study the crosslinking was allowed to reach its saturation value to eliminate tampering. The focus of this work is the effect of temperature on mechanical properties, so the relative results are valuable since the tests were performed using identical degrees of crosslinking.

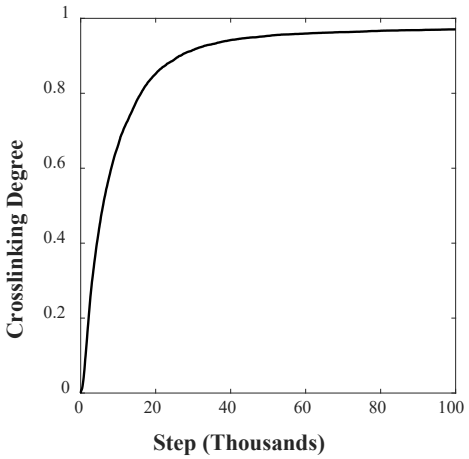

Figure 2. Percent crosslinking as a function of time averaged over the 5 systems, demonstrating asymptotic behavior.

2.3 Unidirectional tensile testing

Prior to the simulated tensile test, each system was copied, and equilibration was performed for 50,000 timesteps for temperatures ranging from 250K to 800K in intervals of 50K for a total 60 distinct simulations. Following equilibration, the systems were subjected to unidirectional tensile deformation at a strain rate of 10^9, a relatively low strain rate for MD, well below the atomic thermal vibration frequencies. The tensile deformation was applied equally to all atoms in the system at a constant engineering strain rate using LAMMPS's fix deform command. The NPT ensemble was employed at the desired temperatures and atmospheric pressure was imposed on the off-loading directions. The virial stresses of each atom were averaged at each timestep to obtain the spatially averaged stress, and these values were averaged over a certain number of timesteps. Although the bulk velocity of the system is ideally null, care was taken to remove the bulk atom motion mean velocity from the kinetic part of the virial stress calculation to better represent the continuum level stresses as detailed in by Subramaniyan et al. [29]. These measures enable the simulation stresses to approach the continuum Cauchy stress, though the strain in the representative unit cell should not be directly compared to macroscopic strains from tensile testing due to MD length-scale incompatibility.

The harmonic potentials of the classical force field do not allow bond breakage to occur; however, the simulations do capture plastic deformation in the form of chain sliding and reorientation, which enables yield strength estimation. The yield strengths were qualitatively compared near the regions where the slopes begin to diminish appreciably. The Young's modulus at each temperature was computed by finding the slope of the linear regression of the initial portion of the stress-strain

curve and averaging over all the randomly seeded systems. The Poisson's ratio was calculated according to the differential definition using the average of the off-axis strains divided by the applied strain. Under the assumption of isotropy for the randomly dispersed CNT system, this data can fully describe the elastic behavior of the material using a single computational experiment. Thermodynamic data was saved from every timestep to reduce random errors caused by system noise.

3. RESULTS

3.1 Temperature effects on strength

In this MD study, thermal degradation mechanisms were limited to variation in strength and stiffness due to increased thermal molecular vibrations. Mass volatilization is another viable measurement for thermal degradation [27], but this was not captured in this study. The classical empirical force field utilized for these simulations does not model bond breakage, so it cannot capture the complete failure of the material; however, it does capture plastic behavior in the form of reorientation and molecule slippage, which causes the stress to plateau as the system is further strained, as shown in Figure 3. There is not a distinctive yield point, but these saturation stress values can be qualitatively correlated to the relative strength of the material, though these values are beyond the strength of the material since the model does not capture bond breakage. Therefore, as expected, the strength of the material degrades as the temperature is increased. This also makes intuitive sense when considering the behavior of the molecular system as the temperature increases; higher temperatures stimulate increased molecular vibration, which increases the likelihood of the system finding configurations with lower potential energy, thereby relaxing some of the stress. As shown in Figure 3, the strength of the system seems to gradually diminish as the temperature increases rather than rapidly decreasing near the Tg.

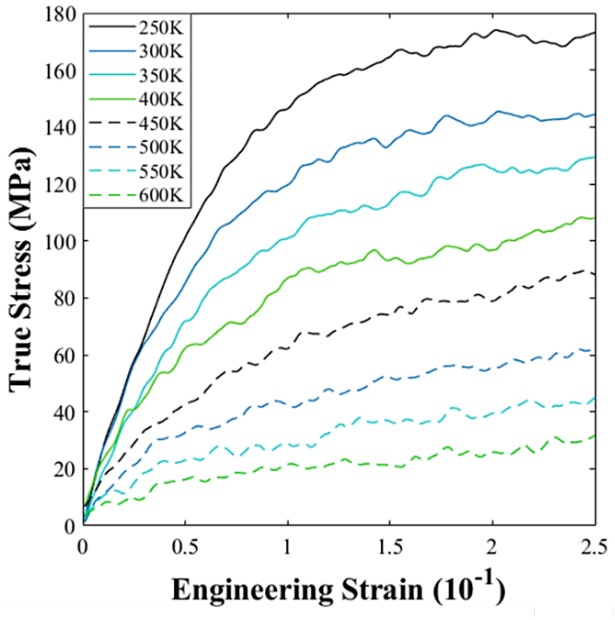

Figure 3. Stress-strain curve for epoxy with randomly dispersed CNTs over a range of temperatures.

The stresses shown in Figure 3 were filtered using the mean values of the averaged system stresses over 250 windowed regions and subsequently regressed using locally weighted scatterplot smoothing (LOWESS), in order to reduce the system noise inherent in finite temperature, moderate strain rate, MD pressure calculations. Although this model does not depict material failure, the nonlinear behavior exhibits a similar curve to the that of the experimental flexural tests performed at room temperature, especially considering the range of their failure strains, up to 8 % strain [30]. Furthermore, the stresses interpolated for room temperature between 5 % and 8 % strain are within range of the strengths measured prior to failure in the same research work (109 – 121 MPa), despite the typical length scale limitations of MD.

3.2 Temperature effects on stiffness

The Young's modulus for each temperature was computed by finding the slope of the linear regression of the initial portion of the stress-strain curve and averaging over all the randomly seeded systems. Similar to the results of the previous section, these stiffness calculations suggest that the thermal degradation in yield strength for this particular polymer is gradual over temperature rather than rapid near the Tg point. From the plot shown in Figure 4, it is difficult to determine the Tg point of the system. However, one can see a slight slope reduction around 450K, which may correspond to the Tg. The values calculated for the Young's modulus near standard temperature are well within the range of the Young's modulus measurements provided by one of the manufacturers of EPON 862 (2.9 – 3.2 GPa) [31] and the values measured by Zhou et al. for EPON 862 epoxy with dispersed CNTs up to 0.4 weight percent (2.54 – 2.75 GPa) [30], lending credibility to computations made in ranges outside experimental data.

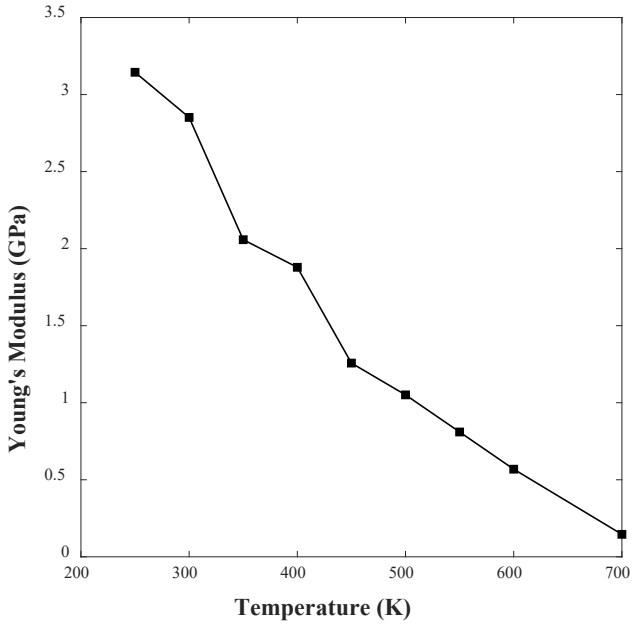

Figure 4. The averaged Young's modulus plotted against temperature.

3.3 Temperature effects on Poisson's ratio

The Poisson's ratio was studied to enable complete definition of the elastic properties using the assumption of isotropy and to investigate the relationship between temperature and the Poisson's ratio for epoxy with randomly dispersed CNTs; Bayar et al. experimentally found that higher temperatures generally correlate to an increasing Poisson's ratio for nanoclay reinforced polymeric nanocomposites [9]. In our systems, the Poisson's ratio was calculated by dividing the average of the off-axis strains by the negative applied strain for every timestep. Figure 5 shows that the Poisson's ratio is initially unsteady over the elastic region, but then settles to a certain value depending on the temperature. The data in Figure 5 is raw data, which indicates that after the initial instability, the MD calculation of the Poisson's ratio remains remarkably stable. The increase in Poisson's ratio with increasing temperature agrees with Bayer et al.'s experiments and can be attributed to the increased molecular mobility. At standard temperature the Poisson's ratio is around 0.4, and then as the temperature increases it approaches 0.5 near the expected Tg corresponding to a liquid-like state. Though, the material can never become a true liquid due to the presence of crosslinks.

In addition we aimed to investigate the role of the Poisson's ratio in the realignment of randomly dispersed CNTs; Feng et al. found that the tendency of randomly dispersed graphene platelets to realign along the loading direction was increased at higher Poisson's ratios [32]. In viewing the molecular trajectories for our highly crosslinked system, negligible CNT realignment was observed. It is expected that with lower degrees of crosslinking, the temperature and Poisson's ratio would have a greater impact on CNT reorientation; although, with small strains and the reduction in strength and stiffness of the matrix due to thermal degradation, any increase in load bearing capability of CNTs due to reorientation would be rendered moot.

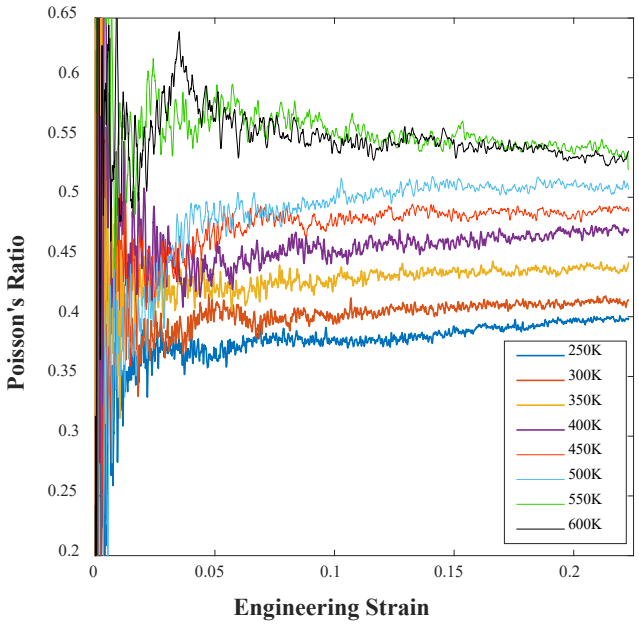

Figure 5. Raw data for the Poisson's ratio as a function of engineering strain for various temperatures.

4. CONCLUDING REMARKS

A molecular model for an epoxy-based polymer composite reinforced by randomly dispersed CNTs was developed, and the effects of temperature on the mechanical properties were investigated using uniaxial MD deformation simulations. Preliminary analysis of the temperature-dependent elastic and plastic response of these nanocomposites indicate that the stiffness and strength gradually degrade as the temperature increases and the increase in temperature is coupled to an increase in the Poisson's ratio. Future work will be performed to study the effects of crosslinking, curing temperature, and CNT weight percentage on the temperature-dependent mechanical properties.

ACKNOWLEDGEMENTS

This research is supported by the Office of Naval Research (ONR), grant number: N00014-17-1-2037. The program manager is Mr. William Nickerson.

REFERENCES

[1] F.-L. Jin, X. Li, and S.-J. Park, "Synthesis and application of epoxy resins: A review," *J. Ind. Eng. Chem.*, vol. 29, (2015), pp. 1–11. http://doi.org/10.1016/J.JIEC.2015.03.026.

[2] A. A. Azeez, K. Y. Rhee, S. J. Park, and D. Hui, "Epoxy clay nanocomposites – processing, properties and applications: A review," *Compos. Part B Eng.*, vol. 45, no. 1, (2013), pp. 308–320. http://doi.org/10.1016/J.COMPOSITESB.2012.04.012.

[3] J. N. Coleman, U. Khan, W. J. Blau, and Y. K. Gun'ko, "Small but strong: A review of the mechanical properties of carbon nanotube–polymer composites," *Carbon N. Y.*, vol. 44, no. 9, (2006), pp. 1624–1652. http://doi.org/10.1016/J.CARBON.2006.02.038.

[4] G. Mittal, V. Dhand, K. Y. Rhee, S. J. Park, and W. R. Lee, "A review on carbon nanotubes and graphene as fillers in reinforced polymer nanocomposites," *Journal of Industrial and Engineering Chemistry*, vol. 21. Elsevier, pp. 11–25, 25-Jan-2015.

[5] N. Subramanian, A. Rai, and A. Chattopadhyay, "Atomistically informed stochastic multiscale model to predict the behavior of carbon nanotube-enhanced nanocomposites," *Carbon N. Y.*, vol. 94, (2015), pp. 661–672. http://doi.org/10.1016/j.carbon.2015.07.051.

[6] A. Kausar, I. Rafique, and B. Muhammad, "Review of Applications of Polymer/Carbon Nanotubes and Epoxy/CNT Composites," *Polym. - Plast. Technol. Eng.*, vol. 55, no. 11, (2016), pp. 1167–1191. http://doi.org/10.1080/03602559.2016.1163588.

[7] A. Allaoui and N.-E. El Bounia, "How carbon nanotubes affect the cure kinetics and glass transition temperature of their epoxy composites? - A review," *Express Polym. Lett.*, vol. 3, no. 9, (2009), pp. 588–594. http://doi.org/10.3144/expresspolymlett.2009.73.

[8] J. P. Foreman, D. Porter, S. Behzadi, P. T. Curtis, and F. R. Jones, "Predicting the thermomechanical properties of an epoxy resin blend as a function of temperature and strain rate," *Compos. Part A Appl. Sci. Manuf.*, vol. 41, no. 9, (2010), pp. 1072–1076.

http://doi.org/10.1016/J.COMPOSITESA.2009.10.015.

[9] L. B. M. Bayar S., Delale F., “Effect of Temperature on Mechanical Properties of Nanoclay Reinforced Polymeric Nanocomposites - Part I: Experimental Results,” *J. Compos. Mater.*, vol. 27, no. 3, (2014). http://doi.org/https://doi.org/10.1061/(ASCE)AS.1943-5525.0000388.

[10] B. Koo, Y. Liu, J. Zou, A. Chattopadhyay, and L. L. Dai, “Study of glass transition temperature (Tg) of novel stress-sensitive composites using molecular dynamic simulation,” *Model. Simul. Mater. Sci. Eng.*, vol. 22, no. 6, (2014). http://doi.org/10.1088/0965-0393/22/6/065018.

[11] D. Qi, J. Hinkley, and G. He, “Molecular dynamics simulation of thermal and mechanical properties of polyimide-carbon-nanotube composites,” *Model. Simul. Mater. Sci. Eng.*, vol. 13, no. 4, (2005), pp. 493–507. http://doi.org/10.1088/0965-0393/13/4/002.

[12] Y. Han and J. Elliott, “Molecular dynamics simulations of the elastic properties of polymer/carbon nanotube composites.” http://doi.org/10.1016/j.commatsci.2006.06.011.

[13] N. Domun, H. Hadavinia, T. Zhang, T. Sainsbury, G. H. Liaghat, and S. Vahid, “Improving the fracture toughness and the strength of epoxy using nanomaterials – a review of the current status,” *Nanoscale*, vol. 7, no. 23, (2015), pp. 10294–10329. http://doi.org/10.1039/C5NR01354B.

[14] L. Martínez, R. Andrade, E. G. Birgin, and J. M. Martínez, “PACKMOL: A package for building initial configurations for molecular dynamics simulations,” *J. Comput. Chem.*, vol. 30, no. 13, (2009), pp. 2157–2164. http://doi.org/10.1002/jcc.21224.

[15] L. Sun *et al.*, “Mechanical properties of surface-functionalized SWCNT/epoxy composites,” *Carbon N. Y.*, vol. 46, no. 2, (2008), pp. 320–328. http://doi.org/10.1016/J.CARBON.2007.11.051.

[16] N. M. O’Boyle, M. Banck, C. A. James, C. Morley, T. Vandermeersch, and G. R. Hutchison, “Open Babel: An open chemical toolbox,” *J. Cheminform.*, vol. 3, no. 1, (2011), p. 33. http://doi.org/10.1186/1758-2946-3-33.

[17] S. Plimpton, “Fast Parallel Algorithms for Short-Range Molecular Dynamics,” *J. Comput. Phys.*, vol. 117, no. 6, (1997), pp. 1–42. http://doi.org/10.1006/jcph.1995.1039.

[18] V. Zoete, M. A. Cuendet, A. Grosdidier, and O. Michielin, “SwissParam: A fast force field generation tool for small organic molecules,” *J. Comput. Chem.*, vol. 32, no. 11, (2011), pp. 2359–2368. http://doi.org/10.1002/jcc.21816.

[19] W. L. Jorgensen, D. S. Maxwell, and J. Tirado-Rives, “Development and testing of the OPLS all-atom force field on conformational energetics and properties of organic liquids,” *J. Am. Chem. Soc.*, vol. 118, no. 45, (1996), pp. 11225–11236. http://doi.org/10.1021/ja9621760.

[20] Axel Kohlmeyer, “TopoTools: Release 1.7.” 2016.

[21] J. R. Gissinger, B. D. Jensen, and K. E. Wise, “Modeling chemical reactions in classical molecular dynamics simulations,” *Polymer (Guildf).*, vol. 128, (2017), pp. 211–217. http://doi.org/10.1016/j.polymer.2017.09.038.

[22] J. W. Sinclair and J. W. Slnclalr, “Effects of Cure Temperature on Epoxy Resin Properties,” *J. Adhes.*, vol. 38, (1992), pp. 219–234. http://doi.org/10.1080/00218469208030456.

[23] H.-V. Nguyen, E. Andreassen, H. Kristiansen, R. Johannessen, N. Hoivik, and K. E. Aasmundtveit, “Rheological characterization of a novel isotropic conductive adhesive – Epoxy filled with metal-coated polymer spheres,” *Mater. Des.*, vol. 46, (2013), pp. 784–793. http://doi.org/10.1016/J.MATDES.2012.11.036.

[24] H. Jin *et al.*, “Fracture behavior of a self-healing, toughened epoxy adhesive,” (2013). http://doi.org/10.1016/j.ijadhadh.2013.02.015.

[25] K. Dušek, “Diffusion control in the kinetics of cross-linking,” *Polym. Gels Networks*, vol. 4, no. 5–6, (1996), pp. 383–404. http://doi.org/10.1016/S0966-7822(97)89914-5.

[26] C. Yang and Z.-G. Yang, “Synthesis of low viscosity, fast UV curing solder resist based on epoxy resin for ink-jet printing,” *J. Appl. Polym. Sci.*, vol. 129, no. 1, (2013), pp. 187–192. http://doi.org/10.1002/app.38738.

[27] F. Carrasco and P. Pagès, “Thermal degradation and stability of epoxy nanocomposites: Influence of montmorillonite content and cure temperature,” *Polym. Degrad. Stab.*, vol. 93, no. 5, (2008), pp. 1000–1007. http://doi.org/10.1016/J.POLYMDEGRADSTAB.2008.01.018.

[28] A. Visco, L. Calabrese, and C. Milone, “Cure rate and mechanical properties of a DGEBF epoxy resin modified with carbon nanotubes,” *J. Reinf. Plast. Compos.*, vol. 28, no. 8, (2009), pp. 937–949. http://doi.org/10.1177/0731684407087560.

[29] A. K. Subramaniyan and C. T. Sun, “Continuum interpretation of virial stress in molecular simulations,” *Int. J. Solids Struct.*, vol. 45, no. 14–15, (2008), pp. 4340–4346. http://doi.org/10.1016/J.IJSOLSTR.2008.03.016.

[30] Y. X. Zhou, P. X. Wu, Z. Y. Cheng, J. Ingram, and S. Jeelani, “Improvement in electrical, thermal and mechanical properties of epoxy by filling carbon nanotube,” *Express Polym. Lett.*, vol. 2, no. 1, (2008), pp. 40–48. http://doi.org/10.3144/expresspolymlett.2008.6.

[31] “General description The EPIKOTE ™ Resin 862/EPIKURE ™ Curing Agent bulletin product EPIKOTE ™ Resin 862/ EPIKURE ™ Curing Agent W System.”

[32] C. Feng, Y. Wang, S. Kitipornchai, and J. Yang, “Effects of reorientation of graphene platelets (GPLs) on young’s modulus of polymer nanocomposites under uni-axial stretching,” *Polymers (Basel).*, vol. 9, no. 10, (2017).

http://doi.org/10.3390/polym9100532.